Atmos. Chem. Phys. Discuss., 10, 2945–2983, 2010
www.atmos-chem-phys-discuss.net/10/2945/2010/

Atmospheric Chemistry and Physics Discussions

This discussion paper is/has been under review for the journal Atmospheric Chemistry and Physics (ACP). Please refer to the corresponding final paper in ACP if available.

Analysis of emission data from global commercial aviation: 2004 and 2006

J. T. Wilkerson[1], M. Z. Jacobson[1], A. Malwitz[2], S. Balasubramanian[2], R. Wayson[2], G. Fleming[2], A. D. Naiman[3], and S. K. Lele[3]

[1]Civil and Environmental Engineering, Stanford University, Stanford, CA, USA
[2]Volpe National Transportation Systems Center, US Department of Transportation, Cambridge, MA, USA
[3]Aeronautics and Astronautics, Stanford University, Stanford, CA, USA

Received: 21 December 2009 – Accepted: 10 January 2010 – Published: 5 February 2010

Correspondence to: J. T. Wilkerson (wilkejt1@stanford.edu)

Published by Copernicus Publications on behalf of the European Geosciences Union.

Abstract

The global commercial aircraft fleet in 2006 flew more than 31 million flights, burned nearly 190 million metric tons of fuel, and covered 38 billion kilometers. This activity emitted substantial amounts of fossil-fuel combustion products within the upper troposphere and lower stratosphere that affect atmospheric composition and climate. The emissions products, such as carbon monoxide, carbon dioxide, oxides of nitrogen, sulfur compounds, and particulate matter, are not emitted uniformly over the Earth, so understanding the temporal and spatial distributions is an important component for modeling aviation climate impacts. Here, we analyze global commercial aircraft emission data for 2004 and 2006. Data, provided by the Volpe National Transportation Systems Center, were computed using the Federal Aviation Administration's Aviation Environmental Design Tool. For both years, analysis of flight data shows 93 percent of fuel was burned in the Northern Hemisphere, 69 percent between 30 N and 60 N latitudes; 77 (75) percent was burned above 7 km in 2004 (2006). This activity led to 177 (162) Tg of carbon from CO_2 globally in 2004 (2006), with half being emitted over three dominant regions: United States, Europe, East Asia. The difference between 2004 and 2006 is a result of fewer flights in 2006 and the methodology used to compute fuel burn and emissions from those flights. We also show that despite receiving only a few percent of global emissions, the Arctic receives a concentration of emissions of the same order of magnitude as the global average. The following is a summary of this data which illustrates the global and regional aviation emissions footprints for 2004 and 2006, and provides temporal and spatial distribution statistics of several emissions constituents. Finally, we show that 87 (85) percent of all flights in 2004 (2006) are short-haul missions, yet those flights are responsible for only 38 (39) percent of total emissions.

ACPD

10, 2945–2983, 2010

Analysis of emission data from global commercial aviation: 2004 and 2006

J. T. Wilkerson et al.

1 Introduction

The following provides an analysis of aviation emissions data for global commercial flights in 2004 and 2006. Previous aircraft emissions inventories have shown that most activity occurs in the Northern Hemisphere mid-latitudes (Baughcum et al., 1996a, b; Kim et al., 2005a; Sutkus Jr. et al., 2001; Eyers et al., 2004; Kim et al., 2007).

Simply scaling data from earlier studies by projected global industry growth rate of 5–7 percent per annum (ICAO, 2007) may not provide emission trends that are representative of geographically varying growth in the aviation sector. For example, India increased its domestic aviation activity by 41 percent in 2005 (MOCA, 2007). As such, it is necessary to continuously update and analyze aircraft emission inventories for use in atmospheric models and policy analysis.

Data for this analysis were provided by Volpe National Transportation Systems Center (Volpe). Here, we provide a brief review of the process for how Volpe assembled the data and provide emission summary statistics for carbon dioxide (CO_2), nitrogen oxides (NO_x), sulfur compounds (SO_x), speciated organic gases, and speciated particle components (black carbon, primary organic matter, and sulfate) from commercial aircraft. We also analyze the vertical profile of emissions, particularly in the upper troposphere and lower stratosphere (UTLS) and emissions in major regions of the world. We further examine the emissions over the Arctic, since it is a particularly sensitive region to climate change. Finally, we compare results with those from previous datasets. We do not examine military aircraft emissions because such emissions are generally not reported or reported separately and not provided; it is estimated that the military contribution is in the range of 10–13 percent of total emissions (Eyers et al., 2004; Waitz et al., 2005).

Aviation emission inventories are important inputs into models examining the climate and pollution effects of aircraft and other anthropogenic emission sources. For example, the inventories discussed here are currently being used in companion studies to examine the effects of aircraft on global climate, atmospheric composition, contrails, and contrail-induced cirrus by treating each aircraft flight at the subgrid scale (Jacobson et al., 2010). It would not be possible to study the effects of subgrid-scale aircraft exhaust plumes and contrails in a global model with an inventory that did not separate emissions by individual flights broken into temporal segments. Due to the large volume of data in such an inventory, it is important to evaluate and summarize the data in a meaningful way. We attempt to do this in the following sections.

2 Methodology

2.1 Global inventory source and description

The United States (US) Federal Aviation Administration (FAA), with support from the Volpe National Transportation Systems Center (Volpe), has developed the Aviation Environmental Design Tool (AEDT) (Roof et al., 2007). The emissions module of AEDT, the System for assessing Aviation's Global Emissions (SAGE), was developed to provide a method for evaluating the effects of various policy, technology, and operational scenarios on aircraft fuel use and emissions. The tool predicts aircraft fuel burn and emissions for all global commercial flights annually, enabling single-flight analysis scenarios, and airport, country, regional, and global scenarios. The module dynamically models aircraft performance, fuel burn and emissions, capacity and delays at airports, and is also capable of providing forecast scenarios. The process for obtaining the flight-level emissions is summarized in-brief below for convenience but is described in greater detail in Kim et al. (2005b) and Kim et al.(2007).

The AEDT inventory provides 4-D flight trajectories (latitude, longitude, altitude, and time) using as much measured data as possible. The data are collected by FAA's Enhanced Traffic Management System (ETMS), which serves as the hub of information. ETMS receives data from several sources, and captures every flight within radar coverage, including scheduled, cargo, military, charter, and unscheduled flights; it also captures every flight that files a flight plan, whether or not the aircraft enters

ACPD
10, 2945–2983, 2010

radar-controlled airspace (Volpe, 2003). ETMS covers all of North America and parts of Western Europe, and records an estimated 50–60 percent of global commercial flights. Additionally, in the 2006 inventory, data collected by EUROCONTROL's Enhanced Tactical Flow Management System (ETFMS) was included. ETFMS provides additional radar-provided schedule and flight data throughout Europe. For the 2004 inventory data, European operations were represented primarily by the Official Airline Guide (OAG), where ETMS coverage did not exist (e.g., in the UK).

When measured data are unavailable or incomplete, the tool refers to the OAG, which lists scheduled passenger flights by participating airlines. The guide represents all US scheduled airlines and the majority of scheduled worldwide airlines. For incomplete ETMS flights and all of ETFMS and OAG flights, trajectories are generated. In 2004, trajectories are generated from statistical distributions of cruise altitudes and horizontal tracks between origination and destination (OD) airport pairs; thus, creating dispersion around the OD Great Circle (GC) estimate. In 2006, the same method is used to determine cruise altitude, but a more accurate "airways track" or flight corridor matching defines the horizontal track between OD pairs. This method determines the shortest distance while traveling along known airways as the horizontal track, which better represents how aircraft typically fly. If a valid airways track does not exist between an OD pair (for instance, airways data between the two airports is non-existent), then a GC track was used. The airways approach has been shown to closely resemble radar data, neglecting reroutes due to adverse weather.

This AEDT emissions inventory is similar to the European AERO2k database. Where AEDT uses ETMS, ETFMS if available, and OAG data as the main components; AERO2k supplements actual flight data with schedule data from the Back Aviation database (fleet registration), and by airspace route structure information (Michot et al., 2004). The agencies that control these databases, FAA and EUROCONTROL, exchange flight-movement information so both databases are expected to improve in accuracy and completeness as collaboration continues.

ACPD
10, 2945–2983, 2010

Once flight trajectories are identified within AEDT and SAGE, each flight is divided into multiple linear segments, or chords. Each chord includes spatial and temporal information for the start and duration of the segment, flight identification information, and pertinent performance parameters such as aircraft and engine type. Each flight may consist of a few dozen chords to several hundred, and the length of each is determined by dynamic parameters such as significant change in speed or altitude, or horizontal deviation.

2.2 Fuel burn and emissions

After the movement database is created, chord-level fuel burn and emissions are calculated. This requires knowledge of takeoff weights, aircraft performance data, and emissions data. Unscheduled and canceled flights account for an estimated 9 percent of all flights and are included by scaling known flights. Validation assessments have shown that SAGE can predict fuel burn to within 3 percent of airline data (Kim et al., 2007). The emissions module then generates estimates of the emissions based on fuel the amount of fuel burned (Table 1). Emissions of CO_2, water vapor (H_2O), and SO_x (modeled as SO_2) follow the fuel burn since they are based strictly on total fuel composition using Boeing-derived emissions indices (EI) (Hadaller and Momenthy, 1993). Emissions of carbon monoxide (CO), hydrocarbons (HC), and NO_x (to a lesser extent) are a function of the individual segment performance so cannot be linearly scaled by total emissions; these species are modeled using Boeing Fuel Flow Method 2 (BFFM2) (Baughcum et al., 1996b; DuBois and Paynter, 2006).

The EI for black carbon particulate matter (PM) used in the 2004 inventory was predominantly the median value of 0.2 g/kg-fuel (S. Lukachko, personal communication, 2007). The PM EI used for the 2006 inventory was 0.035 g/kg, which is more consistent with cruise emissions rather than mean or take-off emissions. Both 2004 and 2006 EI values fall between the low and high range as described by S. Lukachko. Recent work by Volpe and the FAA (Wayson et al., 2009) has advanced the methodology to estimate PM emissions by disaggregating non-volatile PM, from fuel organics and sulfur-related compounds however this is intended for airport operations at ground level conditions rather than cruise-related operations. While the methodology may be applicable at cruise conditions with modifications, this has not been verified.

The PM and gaseous EI predicted by FAA's AEDT are continually improved by analysis of aircraft emissions tests which help characterize exhaust plumes as a function of performance such as during taxi, takeoff, cruise and approach. One such study by The Airport Cooperative Research Program summarized emissions by engine type, thrust, and performance, atmospheric conditions, and plume age (Whitefield et al., 2008). However, like most studies of this nature, this is a ground-based experiment.

We analyzed inventories for 2004 and 2006, which were produced by Volpe using the above methodology. The parameters we used included the beginning and end time, latitude, longitude, and altitude of each flight segment of every flight and the fuel use and emissions of each chemical during the segment. Emission data were prepared in 366 and 365 daily files for 2004 and 2006, respectively, where flight segments, or vectors, were assigned to a specific daily file corresponding to the day of the begin time of the flight. Each annual dataset contains nearly a Terabyte of flight data in this vector format.

The segment data is appropriate for incorporating the emission data in a climate model that treats subgrid emission plumes and contrails and their spreading due to shear and dilution (Jacobson et al., 2010; Naiman et al., 2009); however, the large daily files are too large and cumbersome to load into computer memory. Consequently, these daily files were further divided into hourly files, which provided more manageable file sizes of the same order as the time-scale in the numerical climate study. This resulted in 8784 hourly files for 2004 and 8760 files for 2006. Each hourly file consists of between 200 000 and 600 000 segments depending on specific daily flight activity.

2.3 Vector to grid conversion

Visualizing the flight emissions data enables a better understanding of spatial and temporal characteristics of the emissions. A gridded format, rather than vector format, is

ACPD
10, 2945–2983, 2010

Analysis of emission data from global commercial aviation: 2004 and 2006

J. T. Wilkerson et al.

better suited for visualizing the spatial and temporal distribution of the emissions. For this study, the individual flight data were converted to $0.5^{\circ} \times 0.5^{\circ} \times 0.5$ km spatial gridded data.

Gridding the data required identifying which altitude and horizontal bins the segment intersected and applying the appropriate amount of emissions to each bin. This is accomplished with a three-dimensional parametric vector-plane intercept solution. The distance to the vector intersection with the next longitude, latitude, or altitude plane, based on the chosen resolution, determined the fractional amount of the segment emissions applied to each cell. The solution to each gridded segment was then added to the accumulating global gridded dataset. Once all hourly 3-D gridded arrays were written, the individual hourly files were interrogated for statistics such as emissions during a season, over a particular region or above a given altitude.

2.4 Regional disaggregation

Gridding the data to the desired resolution facilitates a visual inspection of the data both spatially and temporally, and this global footprint illustrates where the emissions generally occur. However, understanding local emissions and local trends enables insight into the regional impacts. The global grid was parsed into regions, and the following describes the two methods used for isolating portions of the global grid.

One method uses the same 19 IPCC regions defined in the IMAGE model (RIVA, 2001) which isolates regions on a 1×1 degree grid resolution. They are identified in Table 2 and illustrated in Fig. 1a. The one-degree resolution was lower than that of the emission data, but allowed for sufficient disaggregation of emissions into logical regions of irregular shapes that roughly matched country or region boundaries.

The second method was to isolate major regions of interest with rectangular bounding boxes. These regions were chosen based on peak aviation activity, such as over the US or the North Atlantic Flight Corridor. These regions are illustrated in Fig. 1b and defined in Table 3.

ACPD
10, 2945–2983, 2010

3 Results

3.1 Global statistics

The global fleet burned 188 Tg of fuel in 2006, which was a decrease of 8 percent from 2004. Figure 2 illustrates where fuel was consumed annually during 2004 and 2006. The annual totals for distance travelled, fuel burned, and emissions constituents are summarized in Table 4. The 2006 inventory was created using an updated version of the AEDT system; thus, some of the differences between 2004 and 2006 can be attributed to modeling improvements made in 2006, and not necessarily actual yearly trends. Nevertheless, several striking features of the emissions distributions are evident from the figures. Nearly all aviation activity occurred in the Northern Hemisphere where almost 93 percent of the fuel is consumed; and nearly 70 percent of the activity occurred in the mid-latitudes of 30–60° N. The decrease in over-all fuel burned from 2004 to 2006 had little effect on hemisphere distributions of emissions, with Northern Hemisphere and Northern mid-latitude percentages remaining about the same in each year.

There is also a noticeable difference in the local distribution of the flight trajectories between the two years; especially over Central Asia and the Atlantic Ocean. As mentioned earlier, when ETMS radar flight data were not available or incomplete, the 2004 inventory employed a dispersion along the great circle to populate the horizontal track, while the 2006 inventory employed a combination of airways track or a direct great circle (when an airways track was not available). Both years included about the same percentage of non-radar tracks. In all, total flight length differed for the two inventory years, with the enhanced methodology employed in 2006 providing shorter distances overall than the methodology employed in 2004. While a global comparison of the difference between methods is not available, recent studies have shown that actual flight paths can increase flight distances an average of 10 percent in Europe and 6–8 percent in the US compared with estimated distances (Kettunen et al., 2005). Considering that half of the included flights are based on the GC, the underestimation of these distances, mostly in Europe, could account for all of the difference between 2004 and 2006 fuel burn estimates. Kettunen further found that 70 percent of the underestimation occurred within the terminal control area of airports; so it is possible that neither the 2004 nor the 2006 inventory methods captured this spatial uncertainty. Consequently, regional comparisons may be more accurate from this analysis than global summaries.

Table 4 also shows differences in emission constituents. Most global totals decreased with the decrease in fuel burn; some proportionately, including CO_2, water vapor, and SO_x. Others, such as NO_x, sulfur, and fuel PM, decreased at twice the fuel reduction rate. However, the data show CO and black carbon emissions changed significantly between 2004 and 2006. The BC decreased 58 percent per annum due to the use of a different EI for black carbon between 2004 and 2006. Globally-averaged CO increased by more than 13 percent per annum. Along with the changes made in horizontal track generation mentioned above, other enhancements were made in AEDT between the 2004 and 2006 inventories.

Specifically pertinent to CO are the enhancements made in terminal-area fuel burn calculations. Even though the fuel burn rate is lower, the highest EI of CO is at low thrust setting, such as during the idle (taxiing operations) or descent portions of flight. While the terminal area represents a proportionately small amount of the overall fuel burn, it represents a substantial portion of the overall CO produced. For the AEDT implementation used in the 2006 inventory, enhancements were made in the calculation of fuel burn in the terminal area. Thus, while the overall fuel burn decreased in the 2006 inventory, changes in terminal area fuel burn calculations could result in the observed increase in CO emissions.

Results from this analysis for 2004 are in general about 9 percent higher than emissions reported for the same year in a previous SAGE inventory report (Kim et al., 2005a). This is primarily due to an improved estimation of unscheduled flights. These reference numbers are shown in Table 5 with units consistent with this study.

ACPD
10, 2945–2983, 2010

3.2 Global CO_2-C emissions

The 2006 dataset describes 31.26 million flights travelling a total of 38.68 billion km, emitting about 162.25 Tg of carbon from CO_2 (CO_2-C). These emissions represent about 2–3 percent of global anthropogenic CO_2 emissions (Sausen et al., 2005). In 2006, the total mean flight was 1237 km and 2.06 h, which is only slightly longer than a flight between San Francisco and Los Angeles. This indicates the dataset is dominated by short-haul flights. One working definition by pilots is short-haul flights are those less than three hours in duration; long-haul flights are those lasting more than six hours; flights lasting between three and six hours are considered medium-haul flights. Aggregating the data by these rules provides the results in Table 6. Short-haul flights indeed represent 85 percent of the total number of flights; this is illustrated in the length-duration plot in Fig. 3, which shows the percentage of flights for a given distance and duration bin. Short-haul flights account for about half of the total annual distance travelled by all commercial aviation and emit 40 percent of the total CO_2-C. Long-haul flights account for less than 4 percent of total number of flights and 21 percent of total distance travelled annually, but also emit about 40 percent of global commercial aviation emissions. Long-haul aircraft must carry the fuel for a longer mission; this weight leads to more fuel burn and twice the rate of emissions of an average short-haul flight.

Figure 4 illustrates annual 2006 carbon emissions from CO_2, which was 2–3 percent of total anthropogenic CO_2 emissions. Not surprisingly, it is very much like the fuel burn footprint for the same year. However, the CO_2 data are presented as emissions per unit area to better understand some of the regional effects described below. Latitude and Longitude zonal profiles are included with the figure. The latitude plot (Fig. 4b) shows the disparity between Northern and Southern Hemisphere emissions, with nearly 2400 kg km^{-2} occurring around 40° N. The longitude plot (Fig. 4c) highlights three regions of significant activity that account for about half of the 162 Tg of global 2006 CO_2-C emissions: the United States, Europe, and Eastern Asia.

ACPD

10, 2945–2983, 2010

All three of these primary regions, and the dominant flight corridors between them, occur in the Northern Hemisphere and almost entirely within northern mid latitudes. Weather circulation patterns in the lower latitudes do not often exchange between the Northern and Southern Hemispheres, and winds in the mid latitudes are typically strong and spread emissions in this region quickly (Zhao and Li, 2006). Thus, since these three regions enjoy the predominant share of aviation activity, they also suffer from the majority of global aviation emissions and subsequent effects.

The provided AEDT flight data and the reduced altitude bins are referenced to mean sea level (MSL). Emissions at altitudes above 7 km m.s.l. can be considered cruise-related emissions, while those below 7 km include shorter flights and local emissions associated and airport activity such as taxi, take-off, and landing. About 75 percent of all aviation fuel was burned above 7 km, where emissions have a longer residence time than those emitted near the surface. The global vertical profile of 2006 CO_2-C emissions (Fig. 5) shows some activity near zero MSL, which is associated with airport activity and take-off/landing. There is a gradual increase in emissions up through 7 km, then a rapid rise above 9 km. Peak emissions occurred between 10–12 km in the upper troposphere and lower stratosphere (UTLS) where contrails predominantly form. An interesting double peak occurs in the UTLS, which can be attributed to East-West and North-South flight clearance altitudes for safe passing.

3.3 Regional CO_2 emissions

Table 7 lists the CO_2-C emissions for each of the IPCC SRES regions for 2004 and 2006, as well as the percent of the regional emissions that occurred above 7 km. These are emissions occurring within the boundaries of each region without regard for origination or destination of the air traffic. Despite covering less than 3 percent of the total surface area (including Alaska), 30 percent of the emissions occurred within the US borders. This is 12 times the globally-averaged emissions per unit area, but it declined by almost 10 percent per year from 2004 to 2006.

ACPD
10, 2945–2983, 2010

Globally, the percent of emissions above 7 km decreased a little between 2004 and 2006. This suggests an increase in short-haul or local flights, but the results shown in Table 6 only partially support this. Most regions contributed to this decrease; however, some, such as Japan, showed both an increase in emissions and a larger percentage emitted above 7 km in 2006, suggesting more over-flights from Asia.

The OECD European region also produces large emissions per unit area, 12 times the global average, although it emits only 15 percent of the global emissions. Emissions within this region only slightly increased from 2004 to 2006. However, in neighboring Eastern Europe, emissions increased 15 percent per year, whereas emissions in the Former USSR exhibited a 10 percent per year decrease. The 2006 inventory included data from ETFMS, which includes Eastern Europe. By including ETFMS (and thus greatly expanding radar-provided schedule and flight data), Eastern Europe was more comprehensively represented in 2006, compared with 2004.

The box regions are slightly larger than similar IPCC regions, which allows for less dependence of results on GC estimation methods. The purpose of these regions is to highlight areas of significant aviation activity. From the global longitudinal profile in Fig. 4c, it is apparent that the continental US receives more emissions than any other region, followed closely by Europe and then Eastern Asia. These three general regions account for only 7 percent of global surface area, but receive over half of all aviation emissions; these regions and selected others are summarized in Table 8.

Unlike the SRES US region, the US box region is essentially the continental US but includes activity surrounding its borders. This region received almost a quarter of all global emissions in 2006, down from 2004. Emissions within the region were dominant in the eastern half of the country, which has more airports and a larger population than the western half. Splitting the region into east and west illustrates the eastern dominance: the Eastern US sub-region receives about two thirds of the emissions with a concentration of more than 11 times the 2006 global average emissions per unit area.

Interestingly, the US region on average falls second in emissions per unit area to Europe. Furthermore, while the US-related emissions declined from 2004 to 2006, European aviation activity increased. Again, this increase in European traffic is a result of including the ETFMS data. There is no evident east-west inflection in the European profile, so this region was not sub-divided. However, the northern part of the region does see slightly more activity.

The East Asia box region has about the same geographical area as the US box, but received about a third of the emissions as the US box region. The activity was predominantly along a Northeast-Southwest orientation. However, China's aviation activity grew at an average of 14.5 percent per year through 2007 (CAAC, 2009). This activity and subsequent emissions within this region are expected to continue to grow over the next few years.

The global footprint also shows two dominant flight corridors: North Atlantic and North Pacific Flight Corridors (NAFC, NPFC). The NAFC box captures the dominant traffic exchange between Europe and the US. The NPFC box covers a larger GC distance so the analysis is less effective when isolated within a single rectangular box. Despite this expansive coverage, however, there are still other regular Pacific flight corridors which were not captured within the box, such as between Japan and Hawaii. Comparing the NAFC and NPFC, more total kilometers were flown within the NPFC bounds, but the NAFC received nearly two times higher concentration of CO_2-C emissions. Also, only a third of the NPFC emissions occurred above 7 km, while nearly all of the NAFC emissions occurred above 7 km.

Another region of interest is the Arctic. While the total emissions over this region were small, about 1.5 and 0.6 percent of the 2004 and 2006 global totals respectively, the emissions per unit area were significant. The polar mean distribution was 115.6 kg km^{-2} in 2004, which was about a third as much as the global average concentration of 347.2 kg km^{-2}. Not only are the emissions on the same order as the global average, but they are spread relatively uniformly throughout the polar region (Fig. 6). All of these emissions occur at altitude where they have a longer residence time than those emitted near the surface. Circulation patterns in the upper mid-latitudes trap polar emissions and push mid-latitude emissions further north (such as those from NAFC)

ACPD
10, 2945–2983, 2010

into the polar region (Forster et al., 2003). Any emissions deposited within or near the Arctic Circle are likely to accumulate over the polar region, which further increases the polar emission concentrations and potential climate impacts on this very sensitive region.

In 2006, the Arctic mean distribution was 53.9 kg km^{-2}, and the 2006 global mean distribution was similar to 2004 at 318.1 kg km^{-2}. The difference in arctic emissions between the two years is likely to be a result of the difference between horizontal track generation. The dispersion along the great circle track generally provides a longer representation of horizontal flight tracks, and the differences between horizontal track modeling techniques may account for most of the difference between 2004 and 2006 polar emissions. Flights between Europe and North America through the NAFC pass close to the Arctic Circle. If a horizontal track does not cross into the polar region, then none of the emissions from any flight along that trajectory can contribute to the region totals. However, if the dispersion method is considered, as in the 2004 data, some of the flights between a given OD pair will pass further north and contribute to the region totals. There are several near-Arctic corridors that can contribute to polar emissions depending on the GC method.

3.4 Temporal distributions

Figure 7a shows the daily global CO_2-C emissions for 2004 and 2006. Since most emissions occurred in the Northern Hemisphere, the annual temporal distribution was dominated by the Northern Hemisphere seasons. Air travel increased in early April and continued through October and dropped off during the winter. The increase in air traffic in summer led to a peak in daily emissions from July through August. Mid-winter activity dropped to a low in January and February. In the 2004 data set, there is an artificial over-count of operations between the months of April and October. This over-count was resolved in 2006 with improvements in the flight schedule creation process. Thus, the 2006 data set more accurately captures the seasonal trends (with peak operation count in the summer months and lowest during the winter months).

The daily emissions curves also show an oscillation illustrating the weekly periodicity. Averaging all emissions by day of the week shows aviation activity peaks on Thursday and Friday and dropped off for the weekend (Fig. 7b).

The daily and weekly profiles were tallied relative to Universal Time Coordinate (UTC), which led to an investigation of emission contributions by the hour. A compilation of the hourly global data results in the 24-h profile in Fig. 7c, which shows annual average emissions per hour. The composite image in Fig. 8 shows the summed annual emissions over each hour of the day, again relative to UTC. Hour 00:00 UTC is midnight in London, and afternoon in Asia where the industry is still very active. Over the next several hours, planes from Asia begin making their way toward Europe and arrive in time for the local morning rush hour. By hour 08:00 UTC, rush hour in Great Britain has ensued and aviation activity over Europe is increasing quickly. 12:00 UTC is 7 a.m. Eastern Standard Time along the US Eastern Seaboard; and aircraft racing across the North Atlantic join an increasing amount of aircraft originating in Eastern US Over the next three hours, the rest of North America begins to add to the aircraft activity as Europe begins to slow down at the end of the work day. Toward the end of the day in the US, aircraft along the east coast begin red-eye flights toward Europe, and aircraft along the pacific coast head out over the pacific toward Asia where the activity starts all over again the next day.

3.5 Other species

In general, other species have the same over-all footprint as CO_2-C. For convenience, NO_x, SO_x, and black carbon are shown in Fig. 9. Unburned fuel or hydrocarbon emissions are assumed to be speciated according to the turbine-engine speciation profile given in Table 9 (Knighton et al., 2009). With this profile, the bulk of hydrocarbon emissions are in the form of ethene, formaldehyde, acetaldehyde, acetylene, propene, C-10 paraffins, C-10 olefins, decanal, dodecanal, benzene, butadiene, and butene, among others. NO_x emissions speciation to NO-NO_2-HONO is assumed to be a function of thrust and engine type (Wood et al., 2008).

ACPD
10, 2945–2983, 2010

4 Summary

We have analyzed global commercial aviation emissions from 2004 and 2006 in total and disaggregated by regions. In 2006, the global commercial aircraft fleet flew 31.26 million flights, burned 188.2 million metric tons of fuel and covered 38.68 billion kilometers. Global 2006 fuel burn and subsequent emissions are generally lower than 2004 results, but this may be in large part due to the difference in horizontal track generation between the two years. However, the global distribution remained about the same for both years: 93 percent of the fuel was burned in the Northern Hemisphere, 69 percent in the northern Mid-latitudes, and 75 percent above 7 km.

The commercial aviation fleet emitted a total of 162 Tg of CO_2-C throughout 2006; the US, Europe and Asia were subjected to about 50 percent of these emissions, despite covering only 7 percent of the global surface area. In general, most regions experienced a small decline in total emissions from 2004 levels, but there was significant growth in Asia and Eastern Europe. The global average for CO_2-C emissions per unit area was 318.1 kg km^{-2} in 2006. The Arctic received only a few percent of the total emissions, but the per unit area emissions was about one fifth of the 2006 global average. Typical wind patterns in the upper mid-latitudes tend to trap these emissions over the arctic and push mid-latitude emissions into the arctic risking significant consequences to this area of high sensitivity to climate change.

Most regions also experienced a decrease in the percent of emissions above 7 km, suggesting fewer fly-over flights or more local short-haul flights. In 2006, an average flight covered 1237 km in 2.06 h, which indicates a dominance of short-haul flights in the annual datasets. Indeed, short-haul flights represented 85 percent of all commercial flights and accounted for about half of the total distance travelled in 2006. These flights indicate a potential for transportation platform switching onto trains or buses. With improved pricing, policies, or incentives, existing transit systems or future high-speed rails may offer a means for offsetting a subset of these flights and the associated emissions.

ACPD
10, 2945–2983, 2010

We have also shown the temporal distribution of emissions on a weekly, daily and hourly basis. The seasonal peak occurred in July and August, with a decrease from November through March. During an average week, peak activity occurred on Thursday and Friday and was slowest on Monday and Tuesday. The hourly distribution of emissions was lowest at about hour 07:00 UTC and quickly ramped up through about 15:00 UTC accounting for Western European and North American rush hours. The hourly emissions remained high until the end of the Asian evening rush around 02:00–04:00 UTC.

Climate impacts from CO_2-C and other greenhouse gas emissions including from aviation are relatively well understood. However, the potential impacts of aviation on climate are unique since most of the emissions occur at altitudes where other anthropogenic sources are absent. The effects of aviation on stratospheric ozone and global climate from persistent contrails and contrail-induced cirrus clouds are potentially significant, but there are large uncertainties in relating aviation emissions to changes in radiative forcing or surface temperature from contrail-associated pathways. Knowing where these emissions occur is the first step in computing the potential impacts. Data presented here support a continuing effort to quantify the effects of aircraft exhaust on climate and global tropospheric air pollution.

Acknowledgements. This work was supported by the Partnership for AiR Transportation Noise & Emissions Reduction (PARTNER) and the Federal Aviation Administration (FAA) under award number DTFAWA-05-D=0006. Any opinions, findings, and conclusions or recommendations expressed in this material are those of the authors and do not necessarily reflect the views of PARTNER or the FAA.

References

Baughcum, S. L., Henderson, S. C., and Tritz, T. G.: Scheduled Civil Aircraft Emissions Inventories for 1976 and 1984: Database Development and Analysis, NASA CR 4722, 1996a.

Baughcum, S. L., Tritz, T. G., Henderson, S. C., and Pickett, D. C.: Scheduled Civil Aircraft

Emissions Inventories for 1992: Database Development and Analysis, NASA CR 4700, 1996b.
General Administration of Civil Aviation in China: China's Airlines to Carry 270 mln Passengers in 2010: http://www.caac.gov.cn/English/News/200708/t20070831_7717.html, access: 19 August 2009.
DuBois, D. and Paynter, G. C.: Fuel Flow Method2 for Estimating Aircraft Emissions, SAE Technical Paper Series, Washington, D.C., 2006-01-198, 2006.
Eyers, C. J., Addleton, D., Atkinson, K., Broomhead, M. J., Christou, R. A., Elliff, T. E., Falk, R., Gee, I. L., Lee, D. S., Marizy, C., Michot, S., Middel, J., Newton, P., Norman, P., Plohr, M., Raper, D. W., and Stanciou, N.: AERO2k Global Aviation Emissions Inventories for 2002 and 2025, QinetiQ Ltd, Farnborough, HampshireQINETIQ/04/01113, 2004.
Forster, C., Stohl, A., and Janmes, P.: The residence times of aircraft emissions in the stratosphere using a mean emission inventory and emissions along actual flight tracks, J. Geophys. Res., 108, 8524–8535, 2003.
Hadaller, O. J. and Momenthy, A. M.: Characteristics of Future Aviation Fuels, in: Transportation and Global Climate Change, edited by: Greene, D. L. and Santini, D. J., American Council for an Energy-Efficient Economy, Washington, D.C., 1993.
International Civil Aviation Organization: Forecasts of Scheduled Passenger Traffic: Long-Term Traffic and Aircraft Movement Forecasts: http://www.icao.int/icao/en/atb/ead/fep/Longterm.htm, 2007.
Jacobson, M. Z., Wilkerson, J. T., Naiman, A. D., and Lele, S. K.: The Effects of Aircraft on Climate and Pollution. Part I: A Model that Treats the Subgrid Evolution of Discrete Size- and Composition-Resolved Contrails from all Commercial Flights Worldwide, in review, 2010.
Kettunen, T., Hustache, J.-C., Fuller, I., Dan, H., Bonn, J., and Knorr, D.: Flight Efficiency Studies in Europe and the United States, 6th USA/Europe Air Traffic Management Research adn Development Seminar, Baltimore, MD, 10, 2005.
Kim, B. Y., Fleming, G. G., Balasubramanian, S., Malwitz, A., Lee, J. J., Waitz, I. A., Klima, K., Locke, M., Holsclaw, C. A., Morales, A., McQueen, E., and Gillette, W.: System for assessing Aviation's Global Emissions (SAGE) Version 1.5: Global Aviation Emissions Inventories for 2000 through 2004, FAA, Ed., Office of Environment and Energy, 48, 2005a.
Kim, B. Y., Fleming, G. G., Balasubramanian, S., Malwitz, A., Lee, J. J., Ruggiero, J., Waitz, I. A., Klima, K., Stouffer, V., Long, D., Kostiuk, P., Locke, M., Holsclaw, C. A., Morales, A., McQueen, E., and Gillette, W.: System for assessing Aviation's Global Emissions (SAGE)

Version 1.5: Technical Manual, FAA, Ed., Office of Environment and Energy, 236, 2005b.
Kim, B. Y., Fleming, G. G., Lee, J. J., Waitz, I. A., Clarke, J.-P., Balasubramanian, S., Malwitz, A., Klima, K., Locke, M., Holsclaw, C. A., Maurice, L. Q., and Gupta, M. L.: System for assessing Aviation's Global Emissions (SAGE), Part 1: Model description and inventory results, Transportation Research; Part D: Transportation and Environment, 12D, 22, 2007.
Knighton, W. B., Herdon, S. C., and Miake-Lye, R. C.: Aircraft Engine Speciated Organic Gases: Speciation of Unburned Organic Gases in Aircraft Exhaust, published as an EPA document as a joint-agency paper, Environmental Protection Agency, Office of Transportation and Air Quality; Federal Aviation Administration (FAA), Office of Environment and Energy, report number EPA-420-R-09-902, available at: http://www.epa.gov/oms/regs/nonroad/aviation/420r09902.pdf, May 2009.
Michot, S., Elliff, T., Fleming, G. G., Kim, B. Y., Holsclaw, C. A., Locke, M., and Morales, A.: Flight Movement Inventory: SAGE-AERO2K, Air Traffic Control Quarterly, 12, 125–145, 2004.
MOCA, India Ministry of Civil Aviation; 2006-07 Annual Report: http://civilaviation.nic.in/reports/an_rep0607eng/Chapter-1.pdf, access: 18 July 2009, 2007.
Naiman, A. D., Lele, S. K., Wilkerson, J. T., and Jacobson, M. Z.: Parameterization of subgrid aircraft emission plumes for use in large-scale atmospheric simulations, Atmos. Chem. Phys. Discuss., 9, 24755–24781, 2009,
http://www.atmos-chem-phys-discuss.net/9/24755/2009/.
RIVA: The IMAGE 2.2 implementation of the SRES scenarios. A comprehensive analysis of emissions, climate change and impacts in the 21st century, National Institute for Public Health and the Environment, Bilthoven, the NetherlandsCD-ROM publication 481508018, 2001.
Roof, C., Hansen, A., Fleming, G. G., Thrasher, T., Nguyen, A., Hall, C., Dinges, E., Bea, R., Grandi, F., Kim, B. Y., Usdrowski, S., and Hollingsworth, P.: Aviation Environmental Design Tool (AEDT) System ArchitectureAEDT-AD-01, 2007.
Sausen, R., Isaksen, I. S. A., Grewe, V., Hauglustaine, D., Lee, D. S., Myhre, G., Kohler, M. O., Pitari, G., Schumann, U., Stordal, F., and Zerefos, C. S.: Aviation radiative forcing in 2000: An update on IPCC (1999), Meteorologische Zeitschrift, 14, 7, 2005.
Sutkus Jr., D. J., Baughcum, S. L., and DuBois, D. P.: Scheduled Civil Aircract Emission Inventories for 1999: Database Development and Analysis, NASA-CR-2001-211216, 2001.
Volpe: Volpe National Transportation Systems Center/US DOT, Enhanced Traffic Management

ACPD
10, 2945–2983, 2010

System (ETMS), Functional Description, Version 7.6VNTSC-DTS56-TMS-002, 2003.

Waitz, I. A., Lukachko, S. P., and Lee, J. J.: Military Aviation and the Environment: Historical Trends and Comparison to Civil Aviation, J. Aircraft, 42, 329–339, 2005.

Wayson, R. L., Fleming, G. G., and Lovinelli, R.: Methodology to Estimate Particulate Matter Emissions from Certified Commercial Aircraft Engines, J. Air Waste Manag. Assoc., 59, 91–100, 2009.

Whitefield, P., D., Lobo, P., Hagen, D., E., Timko, M., T., Miake-Lye, R. C., Taylor, C., Ratliff, G., Lukachko, S., Sequeira, C., Hileman, J., Waitz, I. A., Webb, S., Thrasher, T. G., Oshfeldt, M. R., Kaing, H. K., and Essama, S. G.: Summarizing and Interpreting Aircraft Gaseous and Particulate Emissions Data, Aircraft Cooperative Research Program, Report 9, Transportation Research Board, Washington, D.C., 2008.

Wood, E. C., Herdon, S. C., Timko, M., T., Yelvington, P. E., and Miake-Lye, R. C.: Speciation and Chemical Evolution of Nitrogen Oxides in Aircraft Exhaust near Airports, Environ. Sci. Technol., 42, 1884–1891, 2008.

Zhao, Y. and Li, J.: Discrepancy of mass transport between the Northern and Southern Hemispheres among the ERA-40, NCEP/NCAR, NCEP-DOE AMIP-2, and JRA-25 reanalysis, Geophys. Res. Lett., 33, L20804, doi:10.1029/2006GL027287, 2006.

ACPD

10, 2945–2983, 2010

Table 1. Emissions indices.

Emission factors	2004	2006
H_2O emissions (g/kg-fuel)	1237	1237
CO_2-C emissions[a] (g-C/kg-fuel)	3155.00	3159.00
NO_x-N emissions[b] (g/kg-fuel)	14.52[d]	14.11[d]
CO emissions (g/kg-fuel)	2.57[d]	3.61[d]
SO_x-S emissions(g-S/kg-fuel)	0.6	0.6
HC (as CH_4) emissions (g/kg-fuel)	0.35[d]	0.52[d]
Organic PM emissions (g-C/kg fuel)	0.78	0.015
Sulfur PM emissions[c] (g S(VI)-S/kg-fuel)	0.022	0.012
Black Carbon PM emissions (g-C/kg-fuel)	0.200	0.035

Notes

[a] Reported as 3155 g CO_2/kg fuel for 2004, and 3159 g CO_2/kg fuel in 2006. Carbon from CO_2 obtained by molecular weight ratio: M_C/M_{CO2}

[b] Nitrogen from NO_x obtained by molecular weight ratio: $0.9*M_N/M_{NO}+0.1*M_N/M_{NO2}$

[c] In 2004, 96.3% of the SO_x-S was partitioned to SO_2-S (gas) and 3.7% to S(VI)-S(particle). For 2006, 98% was partitioned to SO_2-S

[d] Effective EI based on total emissions and total fuel burn

ACPD

10, 2945–2983, 2010

Analysis of emission data from global commercial aviation: 2004 and 2006

J. T. Wilkerson et al.

Table 2. IPCC regions (see Fig. 1a for graphical presentation).

	IPCC region	Total area (Thous sqkm)	Percent of total
0	Ocean	327 498	64.21%
1	Canada	12 642	2.48%
2	USA	11 573	2.27%
3	Central America	5354	1.05%
4	South America	20 307	3.98%
5	Northern Africa	6591	1.29%
6	Western Africa	12 203	2.39%
7	Eastern Africa	6985	1.37%
8	Southern Africa	7776	1.52%
9	OECD Europe	6421	1.26%
10	Eastern Europe	1246	0.24%
11	Former USSR	25 157	4.93%
12	Middle East	7110	1.39%
13	South Asia	6068	1.19%
14	East Asia	12 040	2.36%
15	Southeast Asia	9576	1.88%
16	Oceania	13 062	2.56%
17	Japan	948	0.19%
18	Greenland	2715	0.53%
19	Antarctica	14 790	2.90%
	Total	510 061	100.00%

ACPD
10, 2945–2983, 2010

Table 3. Bounds for regional studies (see Fig. 1b for graphical presentation).

	Box region	Total area (Thous sqkm)	Percent of total*
a	United States	14 656	2.87%
b	Eastern US	7361	1.44%
c	Western US	7295	1.43%
d	Artic region	21 152	4.15%
e	Europe	5523	1.08%
f	Eastern Asia	14 925	2.93%
g	North Atlantic flight corridor	11 430	2.24%
h	North Pacific flight corridor	23 571	4.62%

* See Table 1 for Total
[a] 125 W–66 W × 23 N–50 N
[b] 95 W–66 W × 23 N–50 N
[c] 125 W–95 W × 23 N–50 N
[d] North of 66.5 N
[e] 12 W–20 E × 35 N–60 N
[f] 103 E–150 E × 15 N–48 N
[g] 70 W–5 W × 40 N–63 N
[h] 140 E–120 W × 35 N–65 N

ACPD
10, 2945–2983, 2010

Analysis of emission data from global commercial aviation: 2004 and 2006

J. T. Wilkerson et al.

Table 4. Total annual emissions from global commercial aviation.

	2004	2006	Annual growth rate	Index(2004=1)	(Comments)
Distance traveled (Billion km)	41.42	38.68	−3.37%	0.93	
Total number of flights (Million)	33.13	31.26	−2.86%	0.94	
Fuel burned (Tg)	205.68	188.20	−4.34%	0.92	
In Northern Hemisphere	92.7%	92.5%	−0.12%	1.00	(% of Fuel burned)
In Northern Mid-Latitudes	68.9%	69.0%	0.11%	1.00	(30° N–60° N)
H_2O emissions (Tg)	254.42	232.80	−4.34%	0.92	
CO_2-C emissions[a] (Tg)	177.09	162.25	−4.28%	0.92	(C from CO_2)
NO_x-N emissions[b] (Tg)	1.346	1.197	−5.71%	0.89	(N from NO_2-NO mix)
CO emissions (Tg)	0.529	0.679	13.35%	1.28	
SO_x-S emissions[c] (Tg)	0.119	0.111	−3.70%	0.93	(S from SO_x)
HC (as CH_4) emissions (Tg)	0.072	0.098	16.62%	1.36	
Organic PM emissions (Tg)	0.152	0.003[d]	−85.02%	0.02	
Sulfur PM emissions (Tg)	0.014	0.012	−6.38%	0.88	
Black Carbon PM emissions (Tg)	0.0386	0.0068	−58.01%	0.18	

Notes:

[a] Carbon from CO_2 obtained by molecular weight ratio: M_C/M_{CO2}

[b] Nitrogen from NO_x obtained by molecular weight ratio: $0.9*M_N/M_{NO}+0.1*M_N/M_{NO2}$

[c] Sulfur from SO_x obtained by molecular weight ratio: M_S/M_{SO2}

[d] Original 2006 inventory included 0.135 Tg organic PM, modified here to be consistent with BC emissions

ACPD

10, 2945–2983, 2010

Analysis of emission data from global commercial aviation: 2004 and 2006

J. T. Wilkerson et al.

Table 5. Annual emissions reported in previous SAGE study.

	2000	2001	2002	2003	2004
Distance traveled (Billion km)	33.34	31.85	32.60	34.45	37.04
Total number of flights (Million)	29.71	27.67	28.48	28.78	30.38
Fuel burned (Tg)	181	170	171	176	188
H_2O emissions (Tg)	224	210	211	218	233
CO_2-C emissions[a] (Tg)	156.11	146.28	147.10	152.01	162.11
NO_x-N emissions[b] (Tg)	1.131	1.059	1.086	1.122	1.212
CO emissions (Tg)	0.541	0.464	0.480	0.486	0.511
SO_x-S emissions[c] (Tg)	0.073	0.068	0.069	0.071	0.076

Notes:
Data from Kim et al. (2005a)
[a] Carbon from CO_2 obtained by molecular weight ratio: M_C/M_{CO2}
[b] Nitrogen from NO_x obtained by molecular weight ratio: $0.9*M_N/M_{NO}+0.1*M_N/M_{NO2}$
[c] Sulfur from SO_x obtained by molecular weight ratio: M_S/M_{SO2}

Table 6. Flight length and duration for short-haul and long-haul flights.

Global statistics	Totals 2004	Totals 2006	Annual growth rate	Percent of total 2004	Percent of total 2006
Total (100%)					
Distance traveled (Billion km)	41.42	38.68	−3.37%	100.00%	100.00%
Total number of flights (Million)	33.13	31.26	−2.86%	100.00%	100.00%
CO_2-C emissions[a] (Tg)	177.09	162.25	−4.28%	100.00%	100.00%
Avearge flight length (km)	1250.29	1237.19	−0.53%		
Average flight time (h)	1.91	2.06	3.83%		
CO_2-C emissions (kg/km)	4.28	4.20	−0.95%		
Short-Haul (Less than 3 h flight time)					
Distance traveled (Billion km)	22.88	20.85	−4.53%	55.24%	53.92%
Total number of flights (Million)	28.77	26.62	−3.80%	86.84%	85.17%
CO_2-C emissions (Tg)	69.85	64.34	−4.02%	39.44%	39.65%
Avearge flight length (km)	795.31	783.28	−0.76%		
Average flight time (hr)	1.39	1.50	3.87%		
CO_2-C emissions (kg/km)	3.05	3.09	0.53%		
Medium-Haul (between 3 and 6 h flight time)					
Distance traveled (Billion km)	9.52	9.61	0.48%	22.99%	24.85%
Total number of flights (Million)	3.14	3.48	5.26%	9.49%	11.15%
CO_2-C emissions (Tg)	38.51	36.74	−2.31%	21.74%	22.65%
Avearge flight length (km)	3027.52	2759.01	−4.54%		
Average flight time (h)	3.97	3.96	−0.23%		
CO_2-C emissions (kg/km)	4.04	3.82	−2.78%		
Long-Haul (more than 6 h flight time)					
Distance traveled (Billion km)	9.02	8.21	−4.60%	21.78%	21.23%
Total number of flights (Million)	1.22	1.15	−2.60%	3.67%	3.69%
CO_2-C emissions (Tg)	68.74	61.17	−5.67%	38.82%	37.70%
Avearge flight length (km)	7419.18	7117.94	−2.05%		
Average flight time (h)	8.90	9.28	2.08%		
CO_2-C emissions (kg/km)	7.62	7.45	−1.12%		

Notes

[a] Carbon from CO_2 obtained by molecular weight ratio: M_C/M_{CO2}

Table 7. IPCC regional CO_2-C emissions.

	IPCC Region	2004 CO_2-C (Tg)	2004 % total	2004 kg km^{-2}	2006 CO_2-C (Tg)	2006 % Total	2006 kg km^{-2}	Annual growth	CO_2-C above 7 km 2004	CO_2-C above 7 km 2006
0	Ocean	35.05	19.79%	107	29.99	18.48%	92	−7.5%	98.7%	99.2%
1	Canada	9.56	5.40%	756	6.80	4.19%	538	−15.6%	87.6%	87.5%
2	USA	50.72	28.64%	4383	41.77	25.74%	3609	−9.3%	66.6%	65.1%
3	Central America	4.43	2.50%	827	3.26	2.01%	610	−14.1%	66.7%	68.6%
4	South America	5.04	2.85%	248	4.28	2.64%	211	−7.9%	72.2%	68.2%
5	Northern Africa	1.42	0.80%	216	1.57	0.97%	239	5.1%	84.2%	75.7%
6	Western Africa	1.23	0.69%	101	1.21	0.74%	99	−0.8%	83.4%	79.7%
7	Eastern Africa	0.75	0.43%	108	0.76	0.47%	109	0.8%	82.5%	80.6%
8	Southern Africa	1.01	0.57%	130	1.06	0.65%	137	2.6%	74.2%	71.6%
9	OECD Europe	22.52	12.71%	3507	23.95	14.76%	3730	3.1%	63.2%	60.0%
10	Eastern Europe	2.67	1.51%	2146	3.55	2.19%	2847	15.2%	89.8%	86.0%
11	Former USSR	10.22	5.77%	406	8.12	5.00%	323	−10.9%	91.2%	92.3%
12	Middle East	5.35	3.02%	752	6.10	3.76%	858	6.8%	77.1%	71.6%
13	South Asia	3.55	2.01%	586	4.36	2.69%	719	10.8%	81.5%	78.8%
14	East Asia	10.45	5.90%	868	11.70	7.21%	971	5.8%	74.4%	68.3%
15	Southeast Asia	5.50	3.11%	575	5.76	3.55%	601	2.3%	69.4%	63.9%
16	Oceania	3.26	1.84%	249	3.31	2.04%	254	0.8%	71.3%	68.9%
17	Japan	3.86	2.18%	4071	4.45	2.74%	4694	7.4%	55.6%	56.8%
18	Greenland	0.49	0.28%	181	0.25	0.15%	90	−29.4%	99.3%	99.5%
19	Antarctica	0.00092	0.0005%	0.0625	0.00061	0.0004%	0.0415	−18.4%	100.0%	100.0%
	Total	177.09	100.00%	347.20	162.25	100.00%	318.10	−4.3%	77.1%	74.6%

ACPD
10, 2945–2983, 2010

ACPD
10, 2945–2983, 2010

Analysis of emission data from global commercial aviation: 2004 and 2006

J. T. Wilkerson et al.

Table 8. Box region CO_2-C emissions.

	Box region	2004 CO_2-C (Tg)	2004 % Total*	2004 kg km^{-2}	2006 CO_2-C (Tg)	2006 % total*	2006 kg km^{-2}	Annual growth	CO_2-C above 7 km 2004	CO_2-C above 7 km 2006
a	United States	52.05	29.39%	3,552	42.16	23.81%	2877	−10.0%	69.3%	67.5%
b	Eastern US	33.21	18.75%	4511	26.78	15.12%	3,637	−10.2%	65.1%	63.4%
c	Western US	18.84	10.64%	2583	15.38	8.69%	2,109	−9.6%	76.6%	74.7%
d	Artic region	2.44	1.38%	116	1.14	0.64%	54	−31.7%	97.2%	95.2%
e	Europe	21.35	12.06%	3867	23.31	13.16%	4221	4.5%	63.9%	61.7%
f	Eastern Asia	16.23	9.16%	1,087	17.87	10.09%	1197	4.9%	76.0%	71.5%
g	NAFC	13.94	7.87%	1220	11.46	6.47%	1003	−9.3%	96.8%	96.9%
h	NPFC	18.46	10.42%	783	16.00	9.03%	679	−6.9%	34.8%	33.1%
	Total	177.09	100.00%	347.20	162.25	100%	318.10	−4.3%	77.1%	74.6%

* Column does not sum to 100%

Table 9. Speciation profile for emitted hydrocarbons (FAA, 2008).

Species	Mass fraction	Species	Mass fraction	Species	Mass fraction
Ethylene	0.15459	1-Nonene	0.00246	Methanol	0.01805
Acetylene	0.03939	n-Nonane	0.00062	Formaldehyde (FAD)	0.12308
Ethane	0.00521	Isopropylbenzene	0.00004	Acetaldehyde (AAD)	0.04272
Propylene	0.04534	n-Propylbenzene	0.00067	Acetone	0.00369
Propane	0.00078	m-Ethyltoluene	0.00193	Propionaldehyde	0.00727
Isobutene/1-Butene	0.01754	p-Ethyltoluene	0.00080	Crotonaldehyde	0.01291
1,3-Butadiene	0.01687	1,3,5-Trimethylbenzene	0.00068	Butyraldehyde	0.00148
cis-2-Butene	0.00210	o-Ethyltoluene	0.00082	Benzaldehyde	0.00470
3-Methyl-1-butene	0.00140	1,2,4-Trimethylbenzene	0.00438	Isovaleraldehyde	0.00041
1-Pentene	0.00776	1-Decene	0.00185	Valeraldehyde	0.00306
2-Methyl-1-butene	0.00174	n-Decane	0.00320	o-Tolualdehyde	0.00287
n-Pentane	0.00198	1,2,3-Trimethylbenzene	0.00133	m-Tolualdehyde	0.00347
trans-2-Pentene	0.00359	n-Undecane	0.00444	p-Tolualdehyde	0.00060
cis-2-Pentene	0.00276	n-Dodecane	0.00462	Methacrolein	0.00536
2-Methyl-2-butene	0.00185	n-Tridecane	0.00535	Glyoxal	0.01816
4-Methyl-1-pentene	0.00086	C14-alkane	0.00186	Methylglyoxal	0.01503
2-Methylpentane	0.00408	C15-alkane	0.00177	Acrolein	0.02449
2-Methyl-1-pentene	0.00043	n-tetradecane	0.00416	C-10 paraffins	0.14157
1-Hexene	0.00736	C16-alkane	0.00146	C-10 olefins	0.05663
trans-2-Hexene	0.00037	n-pentadecane	0.00173	Decanal	0.05663
Benzene	0.01681	n-hexadecane	0.00049	Dodecenal	0.02831
1-Heptene	0.00438	C18-alkane	0.00002		
n-Heptane	0.00064	n-heptadecane	0.00009	Note:	
Toluene	0.00642	Phenol	0.00726	Conversion factor from THC to TOG	
1-Octene	0.00276	naphthalene	0.00541	(THC is in methane equivalent)	
n-Octane	0.00062	2-methyl naphthalene	0.00206	Turbine	1.1571
Ethylbenzene	0.00174	1-methyl naphthalene	0.00247		
m-Xylene/p-Xylene	0.00282	dimethylnapthalenes	0.00090		
Styrene	0.00309	C4-Benzene + C3-aroald	0.00656		
o-Xylene	0.00166	C5-Benzene+C4-aroald	0.00324		

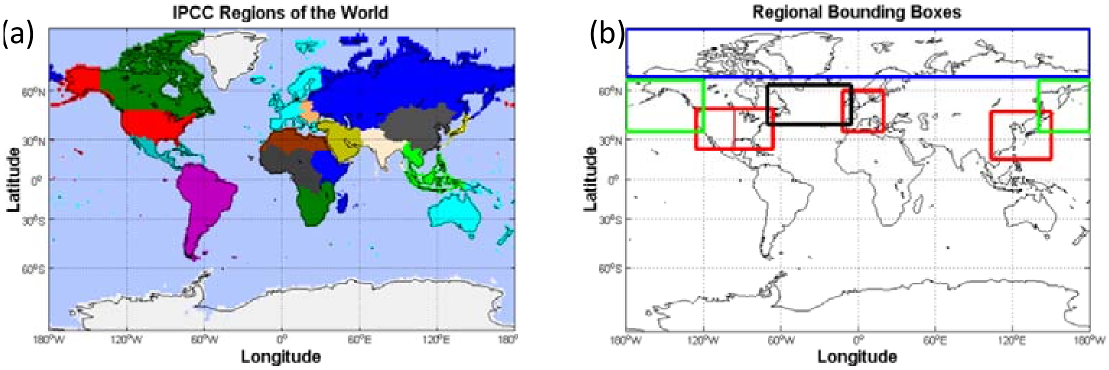

Fig. 1. Regions of the world defined by one of two methods: **(a)** IPCC Regions based on the IMAGE model (RIVA); **(b)** Bounding Box Regions identifying regions of principal activity, including the US, Europe, East Asia, Arctic, and North Atlantic and North Pacific Flight Corridors.

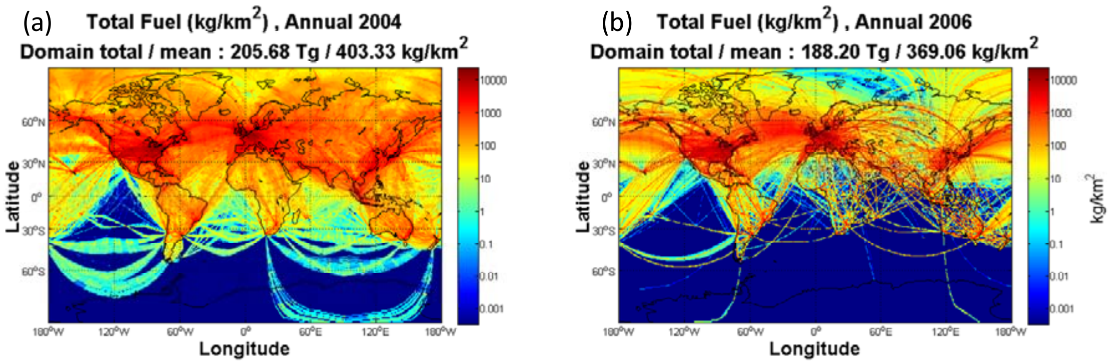

Fig. 2. Spatial distribution of fuel burned in **(a)** 2004 and **(b)** 2006. Nearly all of the emissions occurred in the Northern Hemisphere and about three out of every four grams of fuel was burned in the mid-latitudes. The general distributions were similar between 2004 and 2006; however, the visual differences are an artifact of the different methods of horizontal track estimation used between the two years.

ACPD
10, 2945–2983, 2010

Analysis of emission data from global commercial aviation: 2004 and 2006

J. T. Wilkerson et al.

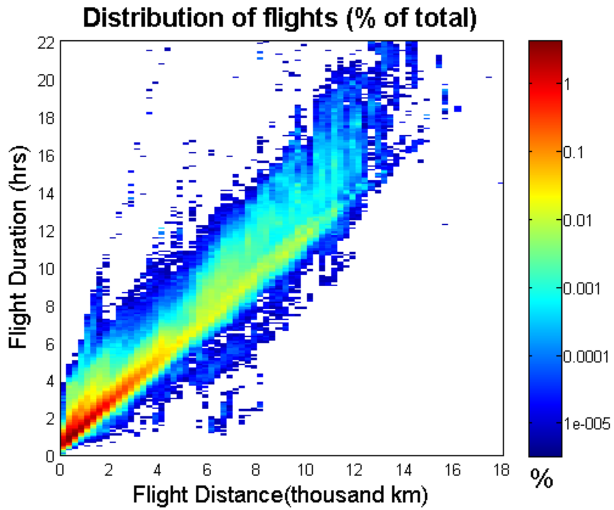

Fig. 3. Percent distribution of all flights for 2006.

ACPD
10, 2945–2983, 2010

Analysis of emission data from global commercial aviation: 2004 and 2006

J. T. Wilkerson et al.

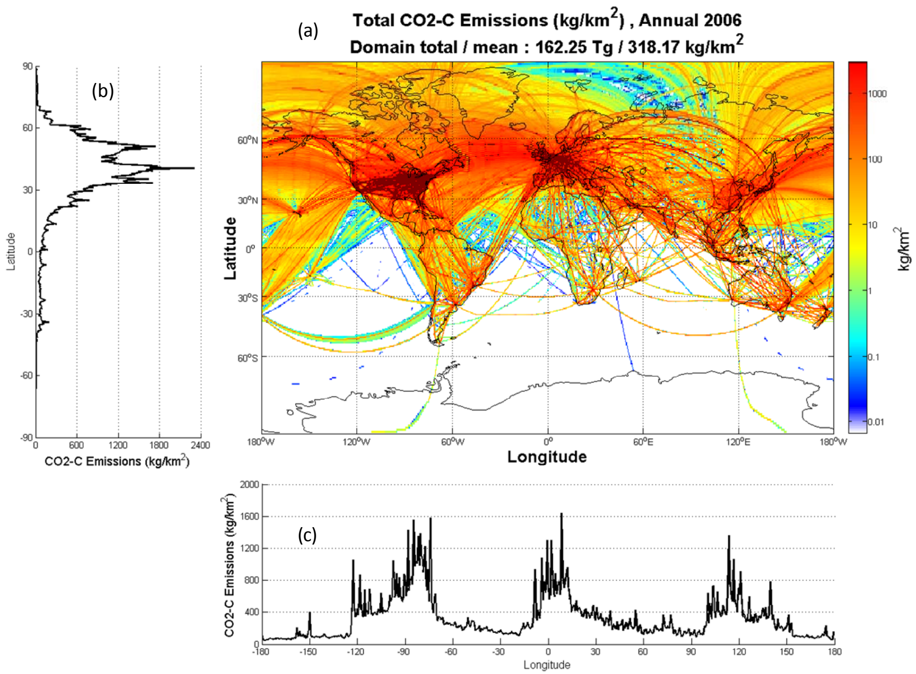

Fig. 4. Spatial distribution of carbon emissions in CO_2. **(a)** Global column total; **(b)** Latitude profile; **(c)** Longitude profile.

ACPD
10, 2945–2983, 2010

Analysis of emission data from global commercial aviation: 2004 and 2006

J. T. Wilkerson et al.

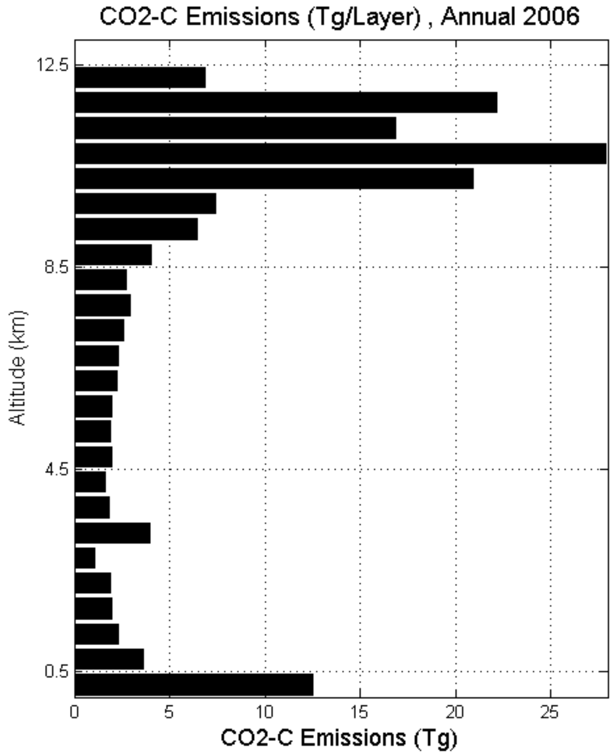

Fig. 5. Altitude profile of annual CO_2-C emissions.

ACPD
10, 2945–2983, 2010

Analysis of emission data from global commercial aviation: 2004 and 2006

J. T. Wilkerson et al.

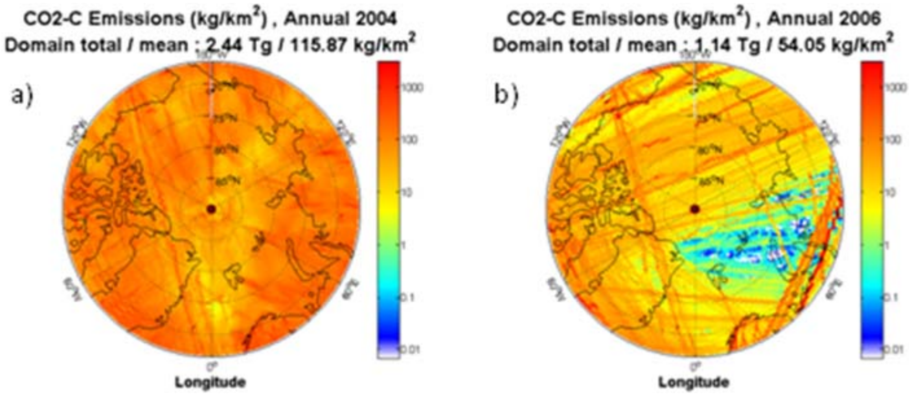

Fig. 6. Arctic aircraft CO_2-C emissions per unit area for **(a)** 2004 and **(b)** 2006.

ACPD
10, 2945–2983, 2010

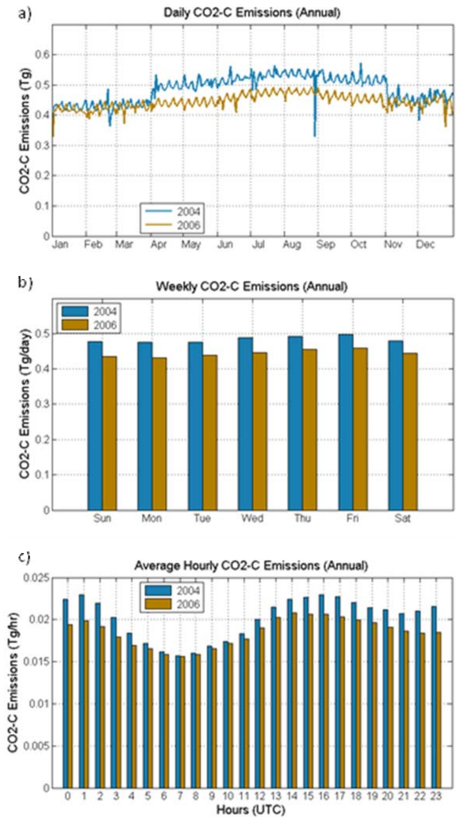

Fig. 7. Annual CO_2-C emissions. **(a)** Total daily emissions, **(b)** total emissions per day of the week, **(c)** average contributions for each hour of the day.

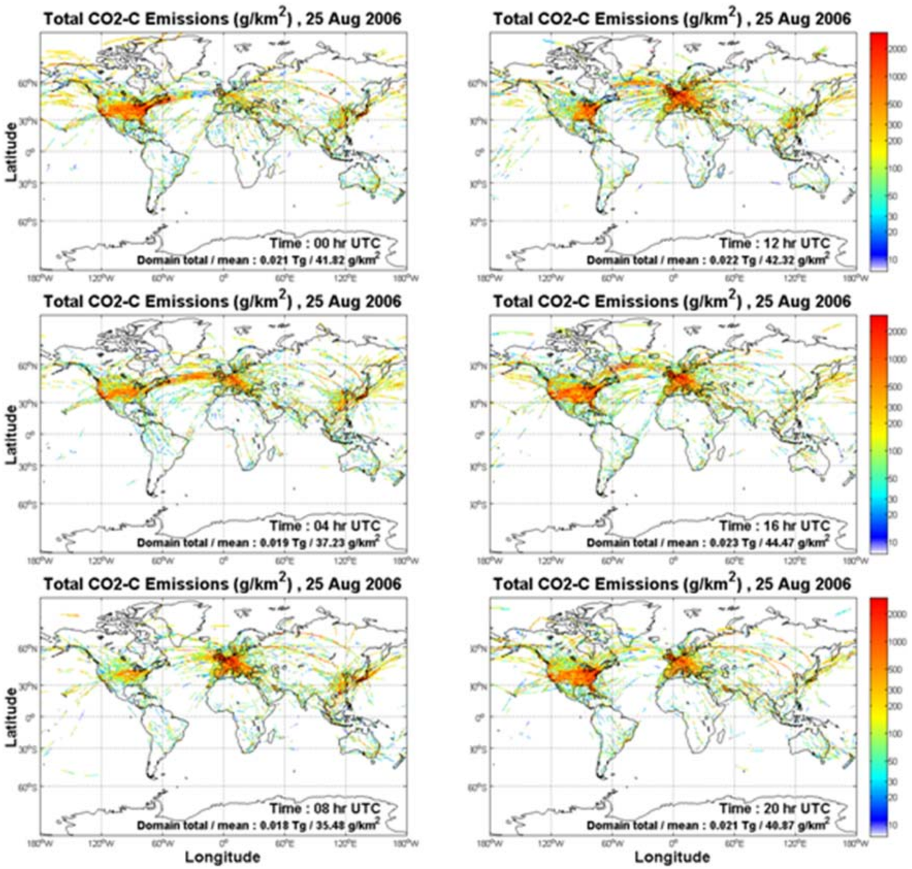

Fig. 8. Composite of hourly CO_2-C emissions through the daily cycle on 25 August 2006. Time is measured relative to UTC. Activity at 00:00 UTC shows evening traffic in Asia. As time progresses, morning rush hours in Europe, then the United States are evident. Toward the end of the day in the US, activity moves over the Pacific toward Asia and redeye flights back to Europe to start the cycle over again.

ACPD
10, 2945–2983, 2010

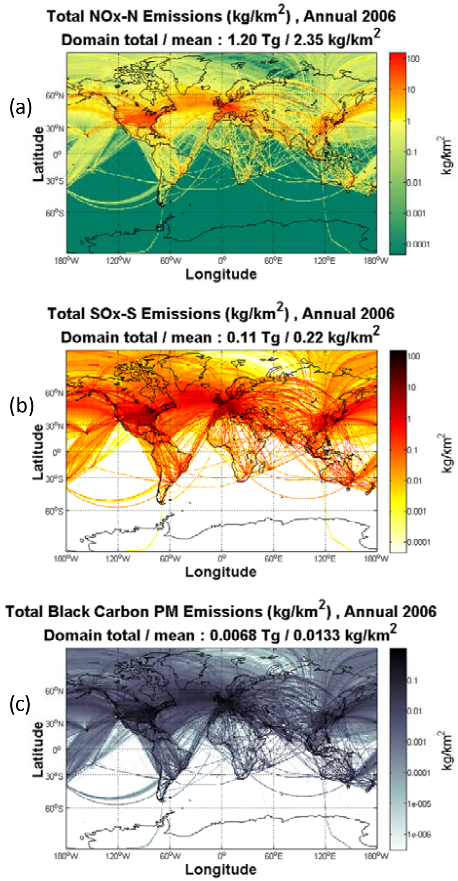

Fig. 9. Global footprint of other species: **(a)** NO_x, **(b)** SO_x, **(c)** Black carbon.

ACPD
10, 2945–2983, 2010

Title Page
Abstract | Introduction
Conclusions | References
Tables | Figures
◀◀ | ▶▶
◀ | ▶
Back | Close
Full Screen / Esc
Printer-friendly Version
Interactive Discussion